A LETTERS JOURNAL EXPLORING THE FRONTIERS OF PHYSICS

August 2008

EPL, **83** (2008) 47006
doi: 10.1209/0295-5075/83/47006

www.epljournal.org

Electrical control of dynamic spin splitting induced by exchange interaction as revealed by time-resolved Kerr rotation in a degenerate spin-polarized electron gas

F. ZHANG, H. Z. ZHENG[a], Y. JI, J. LIU and G. R. LI

State Key Laboratory for Superlattices and Microstructures, Institute of Semiconductors, Chinese Academy of Sciences - P.O. Box 912, Beijing 100083, China

received 27 March 2008; accepted in final form 25 June 2008
published online 6 August 2008

PACS 72.25.Fe – Optical creation of spin polarized carriers
PACS 72.25.Dc – Spin polarized transport in semiconductors
PACS 78.47.-p – Spectroscopy of solid state dynamics

Abstract – Manipulation of the spin degree of freedom has been demonstrated in a spin-polarized electron plasma in a heterostructure by using exchange-interaction–induced dynamic spin splitting rather than the Rashba and Dresselhaus types, as revealed by time-resolved Kerr rotation. The measured spin splitting increases from 0.256 meV to 0.559 meV as the bias varies from −0.3 V to −0.6 V. Both the sign switch of the Kerr signal and the phase reversal of Larmor precessions have been observed with biases, which all fit into the framework of exchange-interaction–induced spin splitting. The electrical control of it may provide a new effective scheme for manipulating spin-selected transport in spin FET-like devices.

The issue of most concern in spintronic devices is how to manipulate the spin degree of freedom in order to obtain superior functionality. The spin-orbit interactions both due to structure asymmetry (Rashba term) and to bulk inversion asymmetry (Dresselhaus term) are going to induce spin splitting at nonzero in-plane wave vectors. They have extensively been explored to manipulate an assembly of spin-polarized electrons in various kinds of prototype spin devices [1]. Because of in-plane momentum dependence, the effective magnetic field, induced by spin-orbit interactions and sensed by an electron spin, varies substantially when the electron is scattered into a different momentum state. This brings a new type of precession-related spin dephasing events [2]. In the present work, instead of the Rashba and Dresselhaus types, it has been demonstrated that a dynamic spin splitting along the growth direction can be induced in heterostructures, when a population imbalance between two electron spin bands is created by circularly polarized excitation. This is because the single-particle energy of an electron will be renormalized due to its exchange interaction with other electrons in interaction electron gas [3]. While such renormalization makes the single-particle energy become smaller and depends on the population, the difference of the renormalized energy between the majority and minority spin bands, *e.g.*, owing to an imbalance between their populations, gives rise to the observed dynamic spin splitting. The electrical control of it has been proved to provide a new effective scheme for manipulating spin-selected transport in spin FET-like devices.

Following the simplest physical picture, magneto-optical Faraday and Kerr effects appear as a result of dynamic bleaching observed in a time-resolved pump and probe measurement configuration. A population imbalance between majority and minority spin bands, created by the circularly polarized pump pulse, makes the optical coefficient of GaAs medium different, as probed with the opposite optical helicities (σ^+, σ^-). We first briefly give the derivation of the Kerr rotation [3,4], which may suitably be used in the case of TRKR measurements. In the reflection configuration, the Kerr angle θ_k and the ellipticity η_k are defined as

$$\theta_k = -\mathrm{Im}\frac{N_+ - N_-}{N_+N_- - 1}, \qquad \eta_k = \mathrm{Re}\frac{N_+ - N_-}{N_+N_- - 1}. \qquad (1)$$

Here, $N_\pm = n_\pm + ik_\pm$ are the complex refraction indexes for two circularly polarized lights $\sigma^\pm$, respectively. The Kerr angle θ_k and the ellipticity η_k can be directly

[a] E-mail: hzzheng@red.semi.ac.cn

related to the real (χ'_{xy}) and imaginary (χ''_{xy}) parts of the off-diagonal matrix elements for dielectric susceptibility χ_{xy} in the form of

$$\theta_K = -\frac{\chi'_{xy}}{n(n^2-1)}, \quad \text{and} \quad \eta_k = -\frac{\chi''_{xy}}{n(n^2-1)}. \qquad (2)$$

From now on, we only consider the specific case, where an ordinary (nonmagnetic) semiconductor is first excited by a circularly polarized pumping pulse, which creates imbalanced density functions $\rho_p^{\pm}$ and $\rho_m^{\pm}$ for two spin-polarized states both in the final up-band p and in the initial low-band m, and is then probed by a linearly polarized probe pulse. By following Kubo formulism [3], one may generalize the matrix element for the dielectric susceptibility $\chi_{\mu\nu}(\omega)$ in the following manner:

$$\chi_{xy}(\omega) = \frac{-i}{4V\hbar}\lim_{\eta\to 0^+}\left\{\sum_{m,p}(\rho_m-\rho_p)_+ \times \frac{|M_+|^2_{mp}}{\omega_p-\omega_m-\omega-i\eta} - \sum_{m,p}(\rho_m-\rho_p)_- \times \frac{|M_-|^2_{mp}}{\omega_p-\omega_m-\omega-i\eta}\right\}. \qquad (3)$$

Here, the density functions are decomposed into spin-majority $(\rho_m-\rho_p)_+$ and spin-minority $(\rho_m-\rho_p)_-$ parts. For an ordinary semiconductor, one has $|M_+|^2_{mp} = |M_-|^2_{mp}$ for the squared matrix elements of the $\sigma^{\pm}$-polarized interband transitions in the vicinity of the band gap. Then, the real part of χ_{xy} is modified as

$$\chi'_{xy}(\omega) = \frac{-\pi}{4V\hbar}\sum_{m,p}(\rho_{p+}-\rho_{p-}) \times |M_\pm|^2_{mp}\delta(\omega_p-\omega_m-\omega). \qquad (4)$$

The summation over the states m in the low-band and the states p in the up-band can be replaced by the summation over k-space, as it is conventionally done to account for the contributions from all the interband transitions, which are allowed by the energy and momentum conservation rule. Eventually, it turns out that in the absence of spin splitting

$$\theta_K = -\frac{\varepsilon'_{xy}}{n(n^2-1)} = \frac{1}{n(n^2-1)}\frac{|M_\pm|^2_{vc}}{16\pi}\left(\frac{2m_r}{\hbar^2}\right)^{\frac{3}{2}} \times\sqrt{\hbar\omega-E_g}\left[\frac{1}{1+e^{\frac{\hbar\omega-E_g-\mu_F^+}{k_BT}}} - \frac{1}{1+e^{\frac{\hbar\omega-E_g-\mu_F^-}{k_BT}}}\right]. \qquad (5)$$

Here, we have assumed that 1) the quasi-equilibrium for both spin-up and spin-down electrons is satisfied so that the original density functions in the conduction band, ρ_{c+} and ρ_{c-}, can be replaced by the respective quasi-Fermi distribution functions with the quasi-chemical potentials of $\mu_F^{\pm}$ (which are measured from the respective bottoms of the majority and minority spin bands) in the conduction band. 2) The effective mass approximation can be justified. Here, $m_r^{-1} = m_e^{*-1} + m_{hh}^{*-1}$; n is the refraction index of the medium. The other quantities are defined as usual.

The above expression clearly describes the important features of KR: the magnitude of θ_k is proportional to $\sqrt{\hbar\omega - E_g}$, obeying the general rule for optical interband absorption. Let us check what happens at $T = 0\,\text{K}$. a) When $\hbar\omega - E_g$ is less than both $\mu_F^{\pm}$, χ'_{xy} and θ_K equal zero; b) When $\mu_F^- < \hbar\omega - E_g < \mu_F^+$, θ_k has a nonzero positive value; c) When $\hbar\omega - E_g$ is larger than both $\mu_F^{\pm}$, χ'_{xy} and θ_k again equal zero. All of these predictions have been in accordance with the experimental observations so far.

However, it is well known that the single-particle energy of an electron will be renormalized due to its exchange interaction with other electrons in interaction electron gas. In the framework of the mean-field theory [3,4], the exchange self-energy is a negative term, and determined by $-\sum_q V_{k-q}(f_q^+ - f_q^-)$, where $V_{|k-q|}$ is the Coulomb interaction between electrons, and f_q is the Fermi distribution function. When the imbalance of the dynamic population in two spin bands is created, say, by the circularly polarized pump pulse in the TRKR measurement, the self-energies for the majority (+) and minority (−) spin bands should also be different, leading to a dynamic spin splitting given by $E_g^- - E_g^+ = |\Delta E_{ex}(k,0)| = -\sum_q V_{k-q}(f_q^+ - f_q^-)$ for the static Coulomb interaction. As a matter of fact, such exchange-interaction–induced spin splitting was also employed to explore its influence on the spin dephasing process in a two-dimensional electron system (2DES) first theoretically [5] and then experimentally [6], as it acts as an effective magnetic field along the growth direction.

Therefore, in the presence of the spin splitting induced by the exchange self-interaction, the Kerr rotation should be expressed in a slightly modified form:

$$\theta_K = -\frac{\varepsilon'_{xy}}{n(n^2-1)} = \frac{1}{n(n^2-1)}\frac{|M_\pm|^2_{vc}}{16\pi\hbar}\left(\frac{2m_r}{\hbar^2}\right)^{\frac{3}{2}} \times\left[\sqrt{\hbar\omega-E_g^+}\frac{1}{1+e^{\frac{\hbar\omega-E_g^+-\mu_F^+}{k_BT}}} - \sqrt{\hbar\omega-E_g^-}\frac{1}{1+e^{\frac{\hbar\omega-E_g^--\mu_F^-}{k_BT}}}\right]. \qquad (6)$$

Equation (6) discloses that KR increases with the population imbalance between the majority and minority spin bands, and switches its sign as long as the population in two spin bands is reversed. It also naturally follows that the variation of the time-resolved Kerr rotation (TRKR) with $\hbar\omega$ could be employed to verify the dynamic band renormalization and the appearance of spin splitting between the majority and minority spin bands.

Based on the idea above, the sample structure in investigation was designed as a single-barrier tunneling diode, grown by molecular beam epitaxy (MBE) with a thick intrinsic GaAs as the absorption layer. The layer structures were grown in the sequence: 250 nm thick Si-doped GaAs buffer layer ($n = 1\times 10^{18}\,\text{cm}^{-3}$) on n^+-GaAs (100) substrate, 200 nm thick intrinsic GaAs, 5 nm thick intrinsic AlAs barrier, 500 nm thick intrinsic GaAs as the

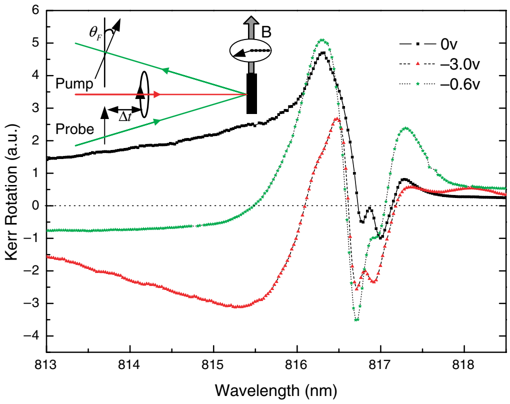

Fig. 1: (Colour on-line) KR was measured at 5 K by simultaneously scanning wavelengths of both pump and probe pulses under different negative biases as the delay time of the probe pulse was fixed at 100 ps.

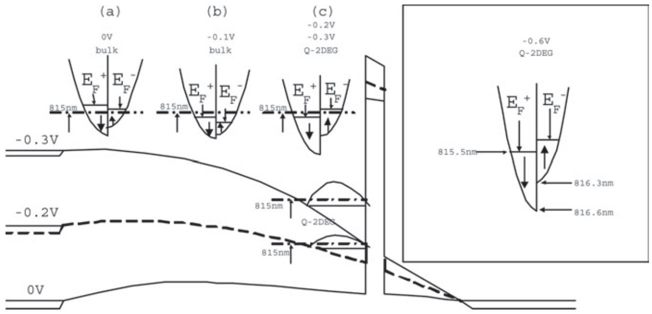

Fig. 2: Band profiles under different negative biases with schematics of majority and minority spin bands plotted against to the photon energy of 815 nm for bulk and quasi-2DEG, the physical content of them as explained in the text. The inset is the plot of majority and minority spin bands at −0.6 V with the labels of the wavelengths at some particular energy positions.

absorption region (labeled as W), 30 nm thick intrinsic $Al_{0.45}Ga_{0.55}As$ and finally covered by a 100 nm thick Si-doped GaAs ($n = 1 \times 10^{18}\,\text{cm}^{-3}$, labeled as L). A $500 \times 500\,\mu\text{m}^2$ optical window was defined by using photolithography and wet etching. An Ohmic contact was formed on the top surface by depositing and alloying Au/Ge/Ni metallic multilayers, the backside contact was formed in the same way on the n^+-GaAs (100) substrate. The sample was mounted inside a magneto-optical cryostat, the temperature of which varied from 1.5 to 300 K and the magnetic field of which scanned up to 10 T.

Optical measurements were performed in a pump and probe configuration (see the inset to fig. 1), using a mode-locked Ti : sapphire laser with a pulse duration of approximately 3 ps and a repetition rate of 76 MHz, in the photon wavelength range from 700 nm to 1000 nm. The pump and probe beams were shined on the sample at an incidence angle of 0° and 5° (with respect to the sample normal) with a spot diameter of about 0.2 mm and the intensities of 1 mW and 0.1 mW, respectively. A negative bias was applied on the top electrode with respect to the back side contact. An electronic feedback circuit programmed and maintained the relative delay time between pump and probe pulses with a temporal resolution of 1.7 ps. In the measurement of scanning wavelength the accuracy of the wavelength is about 0.26 A.

In fig. 1, the KR was measured at a fixed probe delay time of 100 ps under the biases of 0 V, −0.3 V and −0.6 V by scanning the wavelengths of both the pump and probe beams simultaneously. As the wavelength starts to scan from 819 nm, the KR undergoes a first oscillatory change before 816.7 nm. Their overall behavior is roughly the same for 0 V, −0.3 V, −0.6 V, while the amplitude increases slightly with increasing the bias. Since the wavelength range is still below the GaAs band gap, this oscillatory change naturally reflects the lifting of spin degeneracy of the excitons. Such spin splitting has previously been observed in polarized two-dimensional exciton gas, and attributed to the repulsive interaction between excitons due to the Pauli exclusion principle [7]. The small kinks, appearing in the range from 817 nm to 816.6 nm, presumably arise from the spin-split excited levels of the excitons. It should, however, be emphasized that such repulsive interaction applies only for the two-level system with no energy dispersion, like excitons. After the photon energy becomes larger than the band gap (at 816.6 nm for −0.3 V, −0.6 V, and 816.7 nm for 0 V), the KR signals at three biases all reach their own positive maxima, indicating the dominant contribution from the polarized free electron gas in the conduction band. The positive sign is well in accordance with the theoretical expression (1). The most striking feature is that the sign reversal of the KR takes place under the biases of −0.3 V and −0.6 V, after the wavelength goes shorter than 816.1 nm and 815.5 nm, respectively. Meanwhile, the KR under zero bias remains positive over the whole scan range of the wavelengths. Judging from eqs. (5), (6), one has to invoke the fact that only when a spin splitting appears between the majority and minority spin bands with large enough magnitude of $\Delta E_g = E_g^- - E_g^+$, then the quasi-Fermi level E_F^- can be lifted above E_F^+ (E_F^- and E_F^+ are measured from the top of the valence band, and have the relation $E_F^{\pm} = E_g^{\pm} + \mu_F^{\pm}$). As a result, the sign of KR can be reversed on the short wavelength side. For clarity, the conduction bands modified by the exchange interaction are schematically shown in the inset to fig. 2 for the case of 0.6 V only for the sake of illustration. The conduction band edge for E_g^+ should correspond to the cross point at 816.6 nm; E_g^- is assigned to the wavelength of 816.3 nm at the positive peak position; the cross point at 815.5 nm roughly denotes the position of E_F^+. As the wavelength scans from 816.6 nm to 816.3 nm, only the first term in the parenthesis of eq. (6) contributes to the KR in proportion to $\sqrt{\hbar\omega - E_g^+}$. As soon as the wavelength becomes shorter than 816.3 nm, the second term in the parenthesis appears to diminish the KR continuously. The probe beam starts to probe the Kerr response only from the minority spin

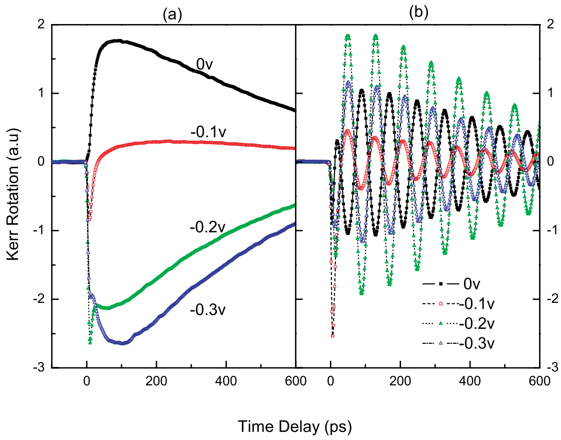

Fig. 3: (Colour on-line) (a) KR was measured at 5 K under different negative biases of 0 V, −0.1 V, −0.2 V, −0.3 V at zero magnetic field as the wavelength is fixed at 815 nm. (b) Larmor precessions were displayed in KR under different negative biases of 0 V, −0.1 V, −0.2 V, −0.3 V at a magnetic field of 2 T, as the wavelength is fixed at 815 nm.

band, as its wavelength becomes shorter than 815.5 nm, leading to the sign reversal of KR. In contrast to the cases of −0.3 V and −0.6 V, the spin splitting induced by the exchange interaction is rather small at the zero bias, so that E_F^- lies always below E_F^+. As a result, the KR always remains positive, and the contribution from the minority spin band only partially cancels that from the majority spin band, as indicated by a sudden drop around 816 nm in fig. 1. Since the delay time of the probe pulse is fixed at 100 ps, the accumulation of the spin-polarized electrons has nearly been completed in the vicinity of the AlAs barrier by drifting away the bulky GaAs layer. Accordingly, the quasi-equilibrium filling in both of the quasi-2D spin bands is almost fulfilled, and the variation of KR with the wavelength approximately reflects the phase-space filling in both spin bands and the spin splitting between them for the case where the photo-excitation is close to the band gap.

To further verify the above point, the temporal transients of the KR were measured at a fixed wavelength of 815 nm under various biases in both the absence and presence of the magnetic field of 2 T in the Voigt configuration. As shown in fig. 3(a), the KR under zero bias shows a positive temporal response, primarily coming from the contribution of the 500 nm thick bulky GaAs layer. A small bias of −0.1 V depresses the positive Kerr signal significantly. That may be ascribed to the fact that the number of spin-polarized electrons, excited in the bulky GaAs layer, decreases due to the fast drifting-off in the electric field. Therefore, KR is substantially suppressed due to the reduction in the filled electron number at the energy probed by 815 nm photons. This may be visualized by comparing fig. 2(b) to fig. 2(a). It is intriguing that the sign of the KR is reversed by increasing the bias to −0.2 V and −0.3 V. In addition, a building-up process in the initial delay time of about 100 ps also appears especially at −0.3 V, indicating that the accumulation of spin-polarized electrons towards the vicinity of AlAs barrier develops under the electric field. Because the Kerr response from the 500 nm thick bulky layer always remains positive as seen from fig. 1, one may reasonably attribute the negative Kerr response at −0.2 V and −0.3 V to the contribution from the quasi–two-dimensional electron gas (Q-2DEG), as depicted by fig. 2(c). In the framework of the above physical picture, the continuously increased accumulation of the spin-polarized electrons, on one hand, lowers both the majority and minority spin bands with respect to the photon energy (at 815 nm) due to the enhancement in the negative exchange self-energy. On the other hand, it eventually makes the dynamic spin splitting large enough to push E_F^- above E_F^+. As long as the photon excitation at 815 nm falls in the gap between E_F^- and E_F^+, the reversal of the KR signal takes place as understood from eq. (6) and illustrated by fig. 2(c).

Similar variations in the phase and amplitude of the Larmor precession are also seen in fig. 3(b) under different biases. It is found that the phase reversal of the Larmor precession takes place early at −0.1 V, implying that the contribution from Q-2DEG is already admixed with that of the bulky layer. Both the phase and the amplitude of the Larmor precession change with the bias in accordance with the sign and the amplitude of the Kerr signal at zero magnetic field.

The abnormal behavior within the initial 40 ps may be attributed to the interference effect because of the drift of the excited spin-polarized electrons towards the AlAs barrier, observed recently by Salis [8]. Since it occurs quite early, it does not affect what concerns us here. Especially, if we trace back to fig. 1, where TRKR is measured in a scanning of wavelength at a fixed delay time (equivalently at a fixed distance of d), the phase factor $\phi = 4\pi nd/\lambda$, which determines the amplitude and phase of the interference, is impossible to vary dramatically, leading a KR sign reversal as the wavelength changes only by less than 0.1 nm.

Although we attribute the phase reversal of the Larmor precession at −0.1 V, −0.2 V and −0.3 V to the dynamic spin splitting appearing between two spin bands of electrons, we still need to discuss some other possible mechanisms. First, it is well known that the dynamic nuclear polarization (DNP) could be induced along the pump beam by polarized optical excitation due to hyperfine exchange interaction between polarized electron spins and nuclear spins. The spin splitting in the conduction band by DNP should display significant difference, when the measurement is performed in the absence and in the presence of magnetic fields, because the Larmor precession in the latter case dephases the electron spin polarization transverse to the applied magnetic field substantially. A time-averaged spin $\overline{S}_\perp$ and its induced effective field will be much smaller than that at zero field by three order of magnitudes [9]. One can never expect that the sign change of the KR in fig. 3(a) takes place synchronously with the phase reversal of the Larmor precession in fig. 3(b) at each of the applied biases. Moreover, our observation persists until a temperature of 125 K, at which DNP should wash away completely. Second, the spin-orbit interactions due to structure and bulk inversion asymmetries (Rashba and Dresselhaus effects), as a well-established mechanism, can induce spin splitting at nonzero in-plane wave vectors. Since the energy interval between the wavelengths of 816.6 nm and 815.5 nm is about 2 meV, it gives an estimated in-plane k-value of $6\times10^5\,\mathrm{cm}^{-1}$, which is very close to the Γ point. If we take the value of Rashba coefficient α as 4 meVÅ for GaAs/AlGaAs heterostructures [10], then the Rashba spin splitting, estimated by $2\alpha K_F$, should be 0.048 meV. This value is much smaller than the values of 0.256 meV (-0.3 V) and 0.559 meV (-0.6 V) we observed in experiment. Thus, the spin splitting from the spin-orbit interaction of the Rashba and Dresselhaus types cannot account for our observed dynamic spin splitting. Moreover, a spin polarization by the in-plane Rashba or Dresselhaus effective field (in k linear approximation) is not detectable by TRKR, which only senses the spin polarization along the optical axis in the perpendicular. Besides, we have carefully checked if any residue Larmor oscillation caused by the in-plane Rashba or Dresselhaus effective field could be observed in the zero magnetic field, as previously seen in [11]. But, nothing is found in fig. 3(a).

In what follows we make a rough estimation for the spin polarization degree and carrier accumulation required for our observation. Again, in the effective mass approximation, the dynamic spin splitting will be estimated by considering only the statically screened 3D Coulomb potential in each spin band. By defining, $p=(n^+-n^-)/(n^++n^-)$, $n=n^++n^-$, one has $n^+=(1+p)n/2$ and $n^-=(1-p)n/2$. Then, the screened Coulomb potential, screening vector and chemical potential are given as follows [3]:

$$V^{\pm}_{|k-q|}=4\pi e^2/[\epsilon_0(|k^{\pm}-q|^2+k^2)],$$
$$k=\sqrt{(6\pi e^2 n)/(\epsilon\mu_F)},$$
$$n^{\pm}=(6\pi^2)^{-1}(2m^*\hbar^{-2}\mu_F^{\pm})^{3/2},$$

where μ_F is calculated from the total carrier density n. For simplicity, the dynamic spin splitting $\Delta E_{ex}(k,T)$, given by $-\sum_q V_{|k-q|}\left(f_q^+-f_q^-\right)$, is estimated at $T=0$ K, then, it becomes

$$\Delta E_{ex}(k,0)=-\left\{\frac{1}{(2\pi^2)}\int_0^{k_F^+}\frac{q^2\mathrm{d}q\sin\theta\mathrm{d}\theta\times4\pi e^2}{\varepsilon_0(k^2+q^2-2kq\cos\theta+\kappa^2)}\right.$$
$$\left.-\frac{1}{(2\pi^2)}\int_0^{k_F^-}\frac{q^2\mathrm{d}q\sin\theta\mathrm{d}\theta\times4\pi e^2}{\varepsilon_0(q^2+\kappa^2)}\right\}. \quad (7)$$

Here, in order to match the measurement, the first integral for the majority spin band should be evaluated at a k-value determined from $k=\sqrt{2m\Delta E_{ex}(k,0)/\hbar^2}$ with $\Delta E_{ex}(k,0)$ being the measured spin splitting, and the second one at $k=0$. Let the following experimental parameters be adopted: the period of laser pulse T is 13 ns, the absorption coefficient α is taken to be $10^4\,\mathrm{cm}^{-1}$, the light power P shone on the sample is about 1 mW. The total density of carrier n is estimated from the excitation power, according to $n=(PT/\hbar\omega V)e^{-\alpha L}(1-e^{-\alpha W})$. By assuming that the degenerate electron gas is confined in a scale of $W^*=150$ nm at -0.3 V, the volume V is taken to be $\pi D^2W^*/4$ with $D=0.2$ mm. An itinerant calculation procedure gives a spin polarization degree p of 28% with a carrier density of $4.0\times10^{15}\,\mathrm{cm}^{-3}$. Next, the same value of p is used in the calculation for -0.6 V. Now, the total carrier density accumulated in the vicinity of the AlAs barrier will be determined in a self-consistent manner. It turns out that $n=1.3\times10^{16}\,\mathrm{cm}^{-3}$, which amounts to a confinement length of 46 nm at -0.6 V. The above estimation is rather rough, but, nevertheless, is instructive and reasonable. It illustrates us how an enhanced accumulation of spin-polarized electron gas can affect the dynamic spin splitting. As a result, we are convinced that the present work shines some light on how one can manipulate the dynamic spin splitting under the circularly polarized photo-excitation by biasing the structure.

In conclusion, by applying bias, spin-polarized electrons, excited by circularly polarized pump pulses in a 500 nm thick intrinsic GaAs layer, are accumulated into the vicinity of an AlAs barrier in a heterostructure. KR, measured as a function of the wavelength at a fixed delay time of 100 ps in a time-resolved pump and probe measurement configuration, reveals the appearance of the dynamic spin splitting between majority and minority spin bands. Both the spin splitting and the phase of the Larmor precession can electrically be controlled. For our case, the spin splitting induced by the exchange interaction increases from 0.256 meV to 0.559 meV as the bias varies from -0.3 V to -0.6 V. In contrast to the Rashba and Dresselhaus types, the exchange-interaction–induced spin splitting is now along the growth direction, and it is more favorable for manipulating spin-selected transport in spin FET-like devices.

* * *

The authors would like to thank Z. C. Niu for the sample growth and P. Xu for the sample processing. This work was in part supported by the National Basic Research Program of China No. 2006CB932801 and No. 2007CB924904, and also by Special Research Programs of the Chinese Academy of Sciences.

REFERENCES

[1] Awschalom D. D. and Flatte M. E., *Nat. Phys.*, **3** (2007) 153.
[2] Cartoix X. *et al.*, *Appl. Phys. Lett.*, **83** (2003) 1462.

[3] Haug Hartmut and Koch Stephan W., *Quantum Theory of the Optical and Electronic Properties of Semiconductors*, (World Scientific Publishing) pp. 149–161.

[4] Sugano S. *et al.*, *Magneto-Optics* (Springer-Verlag, Berlin) 1999, p. 137; Wallis R. F. *et al.*, *Many-Body Aspect of Solid State Spectroscopy* (North-Holland Physics Publishing) 1986, pp. 27–34.

[5] Weng M. Q. and Wu M. W., *Phys. Rev. B.*, **68** (2003) 075312.

[6] Stich D. *et al.*, *Phys. Rev. Lett.*, **98** (2007) 176401.

[7] Viña L. *et al.*, *Phys. Rev. B.*, **54** (1996) R8317; Kimel A. V. *et al.*, *Phys. Rev. B.*, **63** (2001) 235201; Damen T. C. *et al.*, *Phys. Rev. Lett.*, **67** (1991) 3432.

[8] Salis G. and Alvarado S. F., *Phys. Rev. Lett.*, **96** (2006) 177401.

[9] Kikkawa J. M. and Awschalom D. D., *Science*, **287** (2000) 473.

[10] Miller J. B. *et al.*, *Phys. Rev. Lett.*, **90** (2003) 076807.

[11] Brand M. A. *et al.*, *Phys. Rev. Lett.*, **89** (2002) 236601.